Chinese Journal of Polar Science, Vol. 21, No. 2, 180 - 192, December 2010

A coupled regional Arctic sea ice-ocean model: configuration and application

Li Qun(李群)[1*], Zhang Lu(张璐)[1,2] and Wu Huiding(吴辉碇)[1]

1 Polar Research Institute of China, Shanghai, 200136, China

2 The Second Institute of Oceanography, SOA, Hangzhou 310012, China

** E-mail: liqun_hu818@yahoo.com.cn*

Received June 29, 2010

Abstract A regional sea ice-ocean coupled model for the Arctic Ocean was developed, based on the MITgcm ocean circulation model and classical Hibler79 type two category thermodynamics-dynamics sea ice model. The sea ice dynamics and thermodynamics were considered based on Viscous-Plastic (VP) and Winton three-layer models, respectively. A detailed configuration of coupled model has been introduced. Special attention has been paid to the model grid setup, subgrid paramerization, ice-ocean coupling and open boundary treatment. The coupled model was then applied and two test run examples were presented. The first model run was a climatology simulation with 10 years (1992—2002) averaged NCAR/NCEP reanalysis data as atmospheric forcing. The second model run was a seasonal simulation for the period of 1992—2007. The atmospheric forcing was daily NCAR/NCEP reanalysis. The climatology simulation captured the general pattern of the sea ice thickness distribution of the Arctic, i.e., the thickest sea ice is situated around the Canada Archipelago and the north coast of the Greenland. For the second model run, the modeled September Sea ice extent anomaly from 1992—2007 was highly correlated with the observations, with a linear correlation coefficient of 0.88. The minimum of the Arctic sea ice area in the September of 2007 was unprecedented. The modeled sea ice area and extent for this minimum was overestimated relative to the observations. However, it captured the general pattern of the sea ice retreat.

Key words MITgcm, Sea Ice, Arctic Ocean, Regional Model, Climate Change.

doi: 10.3724/SP.J.1085.2010.00180

1 Introduction

Arctic is an important component of the global climate system. Researches in recent years have shown that in the greater context of global warming, more notable changes occurred in the Arctic climate system than other areas over the past 30 years, which have been seen the most intense changes in the past century. Particularly the most notable is the rapid shrinkage of the summer Arctic sea ice extent[1-4] (Fig. 1). The rapid change of sea ice in the Arctic and its prediction has become one

of the hot topics in the research community and the public in recent years[5-6].

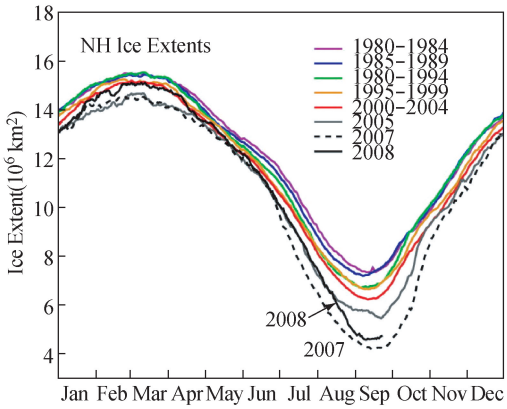

Fig. 1 Daily ice extents of 2005, 2007, 2008 and averaged over the 5-year periods 1980—1984 through 2000—2004[2].

As an important component of the Arctic climate system, sea ice is very sensitive to changes of external forcing such as atmospheric circulation, downward long/short wave radiation and ocean/atmosphere heat flux, etc[7-9]. Slight disturbances of external forcing or initial conditions are highly likely to cause significant changes to the sea ice characteristics such as ice thickness, concentration and other parameters[10-12]. Exactly because of this property of sea-ice, and the status of sea-ice in some key climatic feedback mechanisms, sea-ice plays a determinant role in the Arctic climate system. Also because of the complexity of sea-ice changes, outputs of current sea-ice numerical simulations are subject to considerable uncertainty[13-15]. Therefore, to precisely reproduce the characteristics of sea ice change in recent years and examine its relevant mechanisms using appropriate ice-ocean coupled numerical models with observation results would help to increase predictive capability for future climate changes. Nonetheless, it is still an effective approach in current use to study polar ice, air-sea interactions and climate effects with the help of coupled-system models[12,14,15].

The ongoing project of Estimating the Circulation and Climate of the Ocean, Phase II (ECCO2), which mainly aims to establish a high-resolution global-ocean and sea-ice simulation and diagnostic system, has the improvement of numerical simulation of polar ice-ocean coupled processes as one of its key issues to solve[16]. The project's ocean model is based on MITgcm and its sea-ice model is based on Hibler 79 two-layer thermodynamics model[17], which is significant for understanding polar sea-ice change and its role in climate change. The Arctic regional ice-ocean coupled model described in this paper has mainly been developed on this basis. The basic structure of this paper is: in section 2, the paper gives an overview of the setting of the model and its major parameterization schemes; in section 3, the climatology simulation output and simulation output for summer ice of 2007 are presented; and in section 4, summary and discussion are given.

2 Model Configuration and Related Parameterization Schemes

2.1 The ocean model

The ocean model is based on MITgcm (MIT ocean general circulation model); the Arakawa *C* grid is chosen as the horizontal grid and finite volume difference is used; vertically, the rescaled z coordinate is selected. However, the partial cell is also used to fit as much as possible with topographic boundaries to maintain flux conservation for the model and avoid model drift. The model is designed to simulate large time scale processes such as inter-annual or inter-decadal processes[18]. The ocean model also benefits from the latest developments in physical process parameterization in recent years; in section 2.3, several parameterization schemes frequently used in Arctic ice-ocean coupling and their backgrounds are discussed in more detail.

2.2 Sea-ice model

The sea-ice dynamics processes have been derived from Hibler's viscous-plastic model[17] and the sea-ice thermodynamics based on Winton's [2000] three-layer thermodynamics model[19]. Sea-ice surface heat flux is based on the formula of Parkson and Washington [1979][20]. As conduction heat flux is significantly influenced by ice thickness, in the MITgcm model, calculation of heat flux takes into account sub-grid ice thickness change, i.e. in a horizontal grid, ice thicknesses are categorized into 7 classes, the ice thickness H_n, which are evenly distributed between 5 cm to twice the ice thickness, with $H_n=(2n-1)/7$, $n\in[1,7]$. Ice surface heat flux and albedo changes caused by accumulated snow are considered; snow-ice conversion processes are based on Maksym and Jeffries [2000][21].

2.3 Major model modules

2.3.1 Spherical-cubic grid

Whether for global or regional ocean (or coupled system) numerical simulation, the selection of grid is an important part. In numerical simulation for the Arctic region, there is still the tough problem of the North Pole to tackle. Commonly used approaches include tripole grid (general models such as MOM4, CICE4, etc.) or simply leave out part of the North Pole area. Neither of these approaches essentially solves the singularity problem of the pole. MITgcm adopted a new mesh generation method-the cube sphere grid, which, in combined with finite volume difference, has essentially solved the singularity problem[18] (in addition, when the North Pole problem is not a concern, MITgcm may also use spherical grid or partial linear orthogonal grid).

As a new, effective approach to solving spherical partial differential equations, the cube sphere grid method divides the sphere surface into six identical sections with the central projections of the circumscribed cube. Each section can be covered by a group of arcs of larger circles with equal central angles, so that a quasi-uniform grid

is defined for each section and there is no singularity point in the coordinate system. The corresponding calculation grid is composed of six identical rectangular grids defined by angular coordinate (ξ,η), each between $(-\pi/4,\pi/4)$, so that many intrinsic difficulties in numerical solution of partial differential equations with the common spherical coordinate system are avoided. At the boundaries of the six sections, a grid assembly technology is used to join up the six sections, which allows for stable numerical solution with relative small section overlapping.

In the case of an Arctic regional model, it can be ensured that one of the faces covers most areas north of 50°N, forming a regional curvilinear orthogonal grid, which is just the horizontal grid applied by the Arctic regional ice-ocean coupled model discussed in this paper. Figure 2 shows the cover region and topography of the model, with two open boundaries located in the Bering Sea and the North Atlantic Ocean respectively.

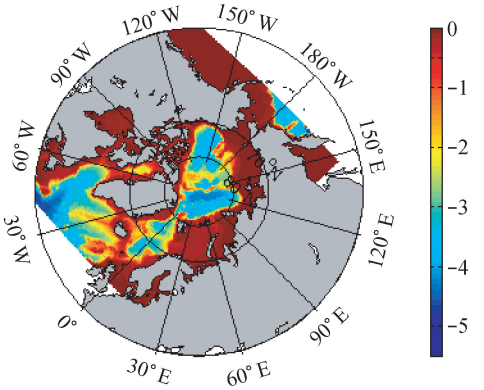

Fig. 2 The regional Arctic Ocean topography (unit: km).

2.3.2 *Selection of vertical coordinate system*

In ice-ocean coupled system, realistic representation of sea ice requires that nonlinear free surface, actual fresh water flux and necessary conservation laws be taken into account. Ice floats in the upper ocean, and as determined by its relative density to sea water, most of its volume is immersed in the upper ocean. If the σ coordinate system is chosen for the numerical simulation, handling of the ice-sea interface would be easier, since this interface, similar to the seabed interface, exactly constitute the top and bottom surfaces of the σ coordinate system, without affecting the vertical stratification of the model. With traditional height coordinates (z coordinate), however, both consideration of the existence of sea ice or effect of the free surface can cause the thinning or disappearance of the upper grid when the top surface is subject to significant undulation (large amplitude fluctuations or sea ice growth to a certain thickness), creating potential factors of instability. Therefore, most z coordinate-based ice-ocean coupled models in current use simplify the state of sea-ice in upper ocean as wholly drift, with upper grid unaffected by thickness of ice; also, virtual salinity flux is used for the ice-sea interface, which is a boundary condition that may cause changes of pressure of water column with freezing and melting of sea ice, creating fake circulation. In fact, no pressure change occurs vertically as sea-ice freezes

or melts.

To deal with this problem, Adcroft and Campin (2003)[22] introduced a rescaled z^* coordinate in MITgcm: $z^* = \sigma(x,y,z,t)H(x,y) = \dfrac{z-\eta(x,y,t)}{H(x,y)+\eta(x,y,t)}H(x,y)$, where $z=H$, representing the seabed; x,y are horizontal coordinate; t is time; η is free surface fluctuation; σ is terrain-following coordinate. In spite of this, z^* is more close to height coordinate. Based on this, Campin(2008)[23] introduced an equivalent free surface $\eta^{eq} = \eta + M_{(ice+snow)}/\rho_w$ to calculate the impact of sea surface fluctuation on sea ice movement.

2.3.3 Parameterization of salt-plume

At the early stage of the sea water freezing, part of the salt is trapped in the ice; and after the forming of sea ice, the salt is gradually released to the sea water. As some studies show, salinity of fresh sea ice may be as high as 20 PSU while after a winter, the salinity of the first-year ice may be 4-6 PSU and salinity of the multi-year ice that has survived at least one summer may be as low as 1-3 PSU. During the whole process, however, distribution of the releasing salt from the sea ice in the upper ocean is uneven, which significantly affects the spatial variability of upper ocean salinity. But generally, in ice-ocean coupled simulation, salt so released was treated simply distributed evenly to the mixed layer.

In the Arctic Ocean, halocline plays an important role in the regulation of heat exchange at the bottom of the mixed layer; besides, it directly affects the energy balance and sea ice mass balance of the ice-ocean coupled system. Accurate depiction of the distribution and evolution of the Arctic Ocean halocline remains one of the difficulties in Arctic ice-ocean coupled simulation. One major issue that compromises such simulation is simplified treatment of the salt freezing-out process by all models. In the ECCO2 project, Nguyen (2008)[25] proposed a parameterization scheme depicting this physical process based on experiment results. Numerical experiments confirm that this scheme has significantly improved depiction of the properties of Arctic Ocean upper ocean water mass. The core of the parameterization scheme lies in the distribution of the discharged salt in upper ocean: instead of simply distributing it evenly as was traditionally practiced, Nguyen (2008)[25] placed the salt on appropriate buoyancy layer as early as possible. When the salt flowing enters a stratified fluid (the plume structure then formed is referred to as salt plume), its depth of penetration and horizontal extent are mainly determined by initial buoyancy, water stratification characteristics and water rotation.

Denote Coriolis force as f, buoyancy frequency as N and buoyancy flux of per unit area of brine as B_0. The relationship between B_0 and volume flux per unit area Q_0 is $B_0 = Q_0 \cdot g\dfrac{\rho_0-\rho_a}{\rho_a}$. In polar oceans, generally stratification effect is dominant, which means $N/f >> 1$. Therefore, the buoyancy depth that the main part of salt plumes can reach is about $z_M \approx (3.0 \pm 1.0)\dfrac{B_0^{1/3}}{N}$, and as soon as these salt plumes reach this depth, they further extend horizontally in all directions. The major part of

ECCO2's salt plume parameterization scheme introduced a vertical distribution function, which provides a 3D depiction of the salt plumes as they develop downward. The function is in the following form:

$$s(z)=\begin{cases} Az^n & if \quad |z|\leqslant|D_{sp}| \\ 0 & if \quad |z|\geqslant|D_{sp}| \end{cases}$$

where n and D_{sp} represent the vertical distribution characteristics and penetration depth of salt plume, respectively and are adjustable parameters in the parameterization scheme. In addition, conservation of salinity should be ensured, which means $S(z)=\int_0^{D_\varphi} s\mathrm{d}z=S_0$, where S_0 is the initial total rejected salt. Based on this conservation relationship, coefficient A could be determined. Based on experiments conducted in the Arctic Ocean, which were compared with observation data, 5 is set for n and D_{sp} is the depth of local mixed layer.

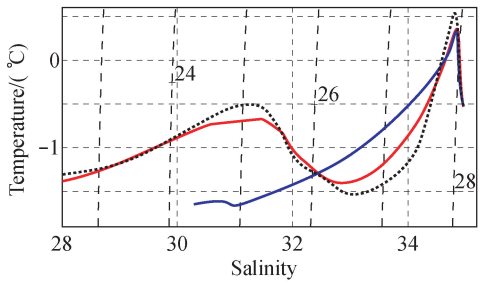

Fig. 3 Comparison of the Salt-Plume parameterization scheme (Dotted line: observation data; Red line: with Salt-Plume parameterization scheme; Blue line: no Salt-Plume parameterization scheme)[25].

2.3.4 *Mesoscale eddies mixing and transport*

Mesoscale eddies play an important role in the transport of physical properties in ocean. However, due to the model resolution limitation, their depiction often relies on some parameterization scheme. Currently, the most often used scheme is the parameterization of eddy-induced velocity related to isopycnal surface thickness diffusion proposed by Gent-McWilliams (1990)[26]. There are two parts to the Redi/GM parameterization of geostrophic eddies. One part aims to realize mix of physical properties by means of a diffusion operator oriented along the local isentropic surface (Redi). The other part adiabatically rearranges physical properties through an advective flux where the advective flux is a function of slope of the isentropic surfaces.

A. The Redi scheme[27]: isentropic surfaces diffusion

Through addition of the term evolution trend in the tracer T (such as temperature, salinity, etc.) equation, the Redi scheme provides tracer diffusion along the isentropic surface. The term of evolution trend is denoted as $\nabla\,\kappa_\rho K_{Redi}\nabla\,T$, where κ_ρ is isopcnal diffusivity, and K_{Redi} is a three-dimensional second rank tensor. Generally, slope of isentropic surfaces in the ocean is very small, i.e. $S_x, S_y << 1$, so the following approximate relationship can be derived:

$$K_{Redi}=\begin{pmatrix} 1+S_x & S_xS_y & S_x \\ S_xS_y & 1+S_x & S_y \\ S_x & S_y & |S|^2 \end{pmatrix}\Rightarrow K_{Redi}=\begin{pmatrix} 1+S_x & 0 & S_x \\ 0 & 1 & S_y \\ S_x & S_y & |S|^2 \end{pmatrix}$$

B. GM parameterization scheme

On this basis, Gent and McWilliams (1990)[26] introduced a component for eddy-induced transport (Cartesian coordinates) in the advection term of the tracer (temperature, salinity, etc.) equation.

$$\frac{\partial T}{\partial t}+(v+v^*)\frac{\partial T}{\partial x}+(u+u^*)\frac{\partial T}{\partial y}+(w+w^*)\frac{\partial T}{\partial z}=R(\kappa_\rho,T)$$

$$v^*=-\frac{\partial}{\partial z}(\kappa_{GM}S_x),\quad u^*=-\frac{\partial}{\partial z}(\kappa_{GM}S_y)$$

$$S_x\equiv-\left(\frac{\partial\sigma}{\partial z}\right)^{-1}\frac{\partial\sigma}{\partial x},\quad S_y\equiv-\left(\frac{\partial\sigma}{\partial z}\right)^{-1}\frac{\partial\sigma}{\partial y}$$

where v^*, u^* are the eddy-induced transport velocity; w^* is derived from continuity equation; κ_{GM} is isopycnal thickness diffusivity. Therefore, in the GM parameterization equation, two issues need to be considered: one is the choice of κ_ρ and κ_{GM}; the other is the calculation of slope of isentropic surfaces. For the second issue, in cases where unstable stratification and areas of intense mixing create infinite slope of isentropic surfaces, the prevailing practice is to assign it a upper limit value. The two coefficients are set as constants, which is acceptable in most cases.

However, in real ocean, eddy movements are considerably uneven temporally and spatially, so its coefficients should also vary temporally and spatially. Visbeck (1997)[28] proposed an uneven mixing coefficient closely related to local baroclinicity. This scheme considers the correlation between κ_{GM} and the state of eddy development and defines κ_{GM} as a function of Eady growth rate $|f|/\sqrt{Ri}$. Its expression is $\kappa_{GM}=\alpha L^2\left\langle\frac{|f|}{\sqrt{Ri}}\right\rangle^z$, where α is a dimensionless constant, L is length scale, and $\langle\,\rangle^z$ represents average depth. The eddy growth rate is average value of depth. $Ri=N^2/(\partial u/\partial z)^2$ is the local Richardson number. Taking into account the thermal wind relationship, the following expression can be derived:

$$\frac{1}{Ri}=\frac{(\partial u/\partial z)^2}{N^2}=\frac{(g\mid\nabla\sigma\mid/f\rho_0)^2}{N^2}=\frac{M^4}{|f|^2N^2}$$

Define $M^2=\frac{g}{\rho_0}|\nabla\sigma|$ and substitute it into the κ_{GM} expression, there is $\kappa_{GM}=\alpha L^2\frac{|M^2|^Z}{N}=\alpha L^2\langle|S|N\rangle^z$.

Chose length scale L as the first baroclinic Rossby deformation radius, i. e. $L=\lambda_R=\frac{1}{f}\int Ndz$. In addition, the expression incorporates a depth-averaged process. In actual operation, choice of depth is subject to considerable uncertainty, often limited to above 1000m; and κ_{GM} decreases as depth increases because baroclinic eddy movements are less active in the deep ocean.

In the Arctic Ocean, the Pacific inflow plays an important role in the Western Arctic Ocean water mass' formation and ocean circulation. However, due to scarcity of observation data, study on the role of the Pacific inflow in the Arctic Ocean transport process and its impact on sea ice change is not very in-depth and mostly based on the ap-

plication of coupled models. The Arctic Ocean Model Inter-comparison Project (AOMIP) has brought together major Arctic regional ice-ocean coupled models from the related research groups. After several years of development, researchers have obtained fairly deep understanding of the Arctic Ocean circulation system and sea ice variability characteristics; however, they also begin to realize the weak points in current models[24]. One of these is that the depiction of the route of the Pacific inflow's transport in the western Arctic Ocean, especially when it enters the Canadian Basin, is far from accurate. All models with no exception underestimate transport of Pacific water into the Canadian Basin, compromising the accurate depiction of fresh water volume of the whole basin.

Further researches showed that the main cause of these issues lies in inaccurate parameterization of mesoscale eddies. Maslowski et al (2008)[29] concluded through comparative experiments that under the same mesoscale eddy parameterization scheme, low-resolution models significantly underestimate Antarctic Ocean mesoscale eddy movements. Through coupled model simulation with an eddy-resolving system, Watanabe (2008)[30] studied the Arctic Ocean salinity bias problem of previous existing models. He concluded that one of the major causes is the underestimation of the transport of the Pacific inflow into the Canadian Basin by existing models, which also leads to overestimation of Pacific Ocean water flowing into the Eurasian Basin, resulting in that salinity in the Eurasian Basin is on the low side. After introduction of Visbeck (1996)'s variable eddy coefficient parameterization scheme, the simulation results can be significantly improved[30].

2.4 Coupling Process

The model described in this paper is an ice-ocean coupled system. As diagrammed by Figure 4, atmospheric forcing fields, which use NCEP reanalysis data, are input to drive the system. The system mainly needs the following atmospheric data (NCEP data provided four times daily; 1992-2002 average was used for climatology): a. 2 m atmosphere temperature field; b. 2 m atmosphere humidity field; c. 10 m wind speed data (u,v); d. precipitation; e. long/short-wave radiation, etc. The model takes into account the effect of runoff. Due to lack of data, however, in the subsequent numerical experiments, results of monthly climatology variation were used for runoff data.

In the system, ice and ocean are coupled bidirectionally, with the ocean module providing surface temperature, salinity, flow field information to the ice module, and the ice module providing information on ice concentration, fresh water flux as the result of ice melting, heat flux, etc.

3 Preliminary Model Result

3.1 Experiment Configuration

In regional climate simulation, the handling of open boundaries is a difficult issue. In the Arctic regional ice-ocean coupled model described in this paper, the open

boundary conditions come from MITgcm's global integration experiment CS510. In the experiment, the vertical coordinates adopted the aforesaid rescaled height coordinates and fully nonlinear free-surface was used. The standard experiment result published by ECCO2 was still based on the original topographic elevation coordinates. In addition, in the experiment, the salt plume parameterization scheme is used (for specific parameters, see Nguyen (2008)[25]); GM90 and Visbeck's variable coefficient scheme is used for the mesoscale eddies parameterization.

The experiment described in this paper can be divided into the following steps: firstly, the model is driven for 50 years using climatology NCEP (1992-2002 average) data. On this basis, integration result of the 50th year is analyzed as the steady state of climatology simulation. Secondly, with integration result of the 50th year used as initial state, the model is driven for 10 years by NCEP daily forcing field of 1992. Then integration is performed from 1992 to 2007, and the integration result of 2007 is compared with some observation data for analysis.

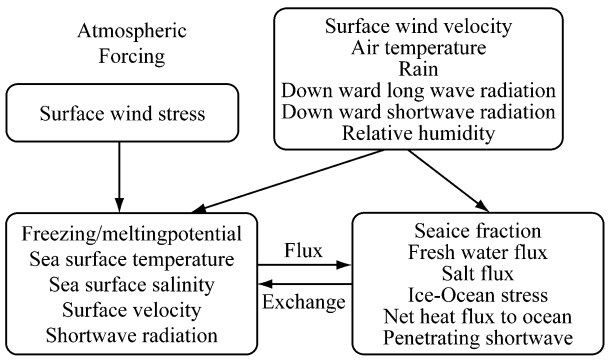

Fig. 4 The Sea ice-ocean coupled system.

3.2 Climatology results and analysis

Figure 5 shows the spatial distribution of the Arctic summer and winter sea-ice thickness of the 50th year of climatology forcing. Overall, the result reveals the basic pattern of Arctic sea ice thickness distribution, i. e., the Canadian Archipelago and northern Greenland have greater sea ice thickness all the year round, while ice thickness along the Siberian coast, whether in winter or summer, is much smaller. Another typical characteristic is that virtually the whole Barents Sea is free of sea-ice coverage all the year round, which is related to the northward heat transfer from the North Atlantic Ocean. Both observation and numerical studies show that most of the heat from the Atlantic Ocean deposited in the Barents Sea, resulting this area above-freezing-point surface temperature despite its high latitudes.

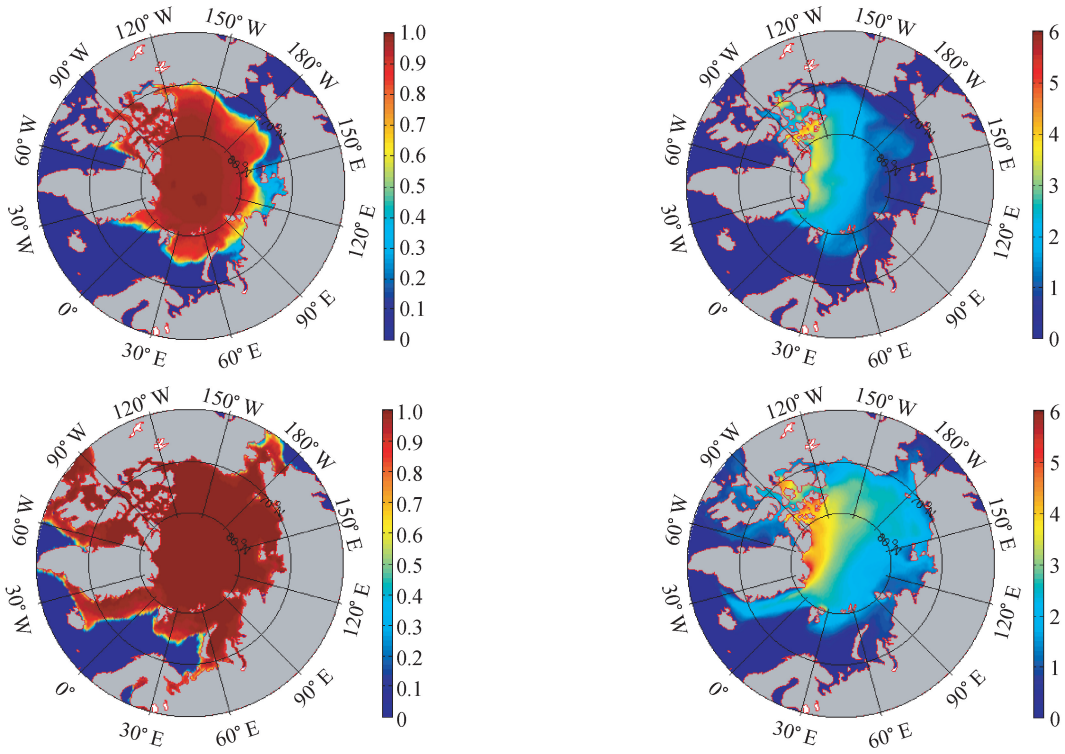

Fig. 5 Averaged summer and winter Arctic sea ice thickness distribution(Units: m).

Figure 6 compares the observation data and our numerical calculations for 1992-2007 September Arctic sea ice extent anomalies. As the curves indicate, simulation result and observation data are considerably correlated ($R^2 = 0.88$). The simulation output basically reflects Arctic summer sea-ice extent anomalies over the 16 years. Although simulation result between 2005 and 2007 is higher than observation data, the drastic decrease of sea ice extent in 2007 is clearly shown (Fig. 7) that the year had the smallest ice extent of the 16 years as observation data shown. In addition, the Arctic sea ice extent minimum in 2002 and 2005 is also accurately depicted.

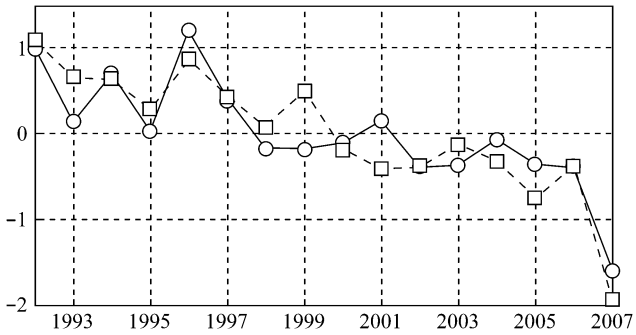

Fig. 6 1992-2007 September average sea ice extent anomaly (Dashed: model result; solid line: observation data from NSIDC, unit: million km^2).

3.3 Simulation result of the 2007 Arctic sea ice minimum

Figure 7 shows the summer ice concentration and thickness distribution of 2007 (average in September) calculated with the model driven by NCEP daily wind field. The blue line represents edges of sea ice obtained through SSMI satellite observation data; the white line represents model result. As shown in Figure 7, the numerical simulation has basicallycaptured the summer sea ice distribution of the year; as shown by thickness distribution, compared with climatology result, extent of sea ice with thickness above 4 m significantly decreased in the summer of 2007. In quantitative term, however, the model result overestimates the average ice extent for September 2007, which is mainly seen at 150°W-120°E, 75°N-85°N in the Pacific sector and small sea areas between the oceanic area and the Barents Sea. The result is basically consistent with the simulation result of Lindsay et al (2009)[15]. The author believes that this is perhaps due to the NCEP data selected in the model, which do not support precise depiction of high latitude wind field characteristics.

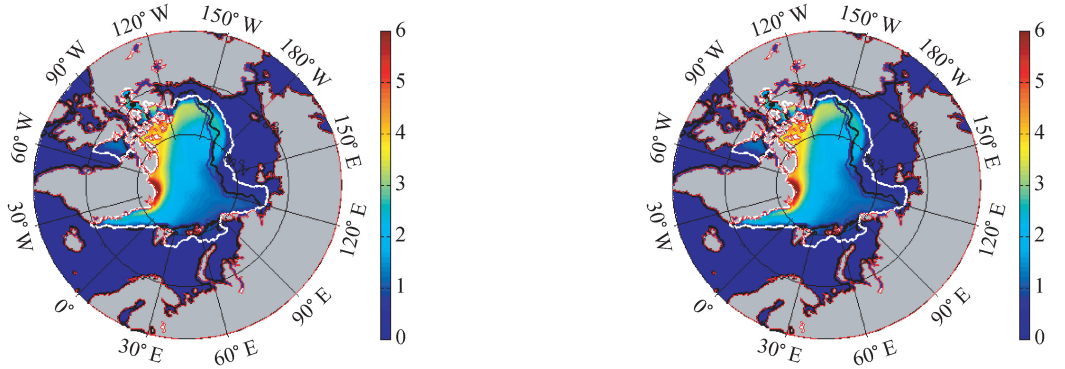

Fig. 7 2007 September averaged sea ice concentration (left) and thickness (right)(Blue: observed sea ice edge; white: modeled sea ice edge. Unit: m).

4 Conclusion

The paper describes an ice-ocean coupled model for the Arctic Ocean. Its ocean model is based on the MITgcm; while the coupled sea-ice model has been developed with reference to Hibler's thermodynamic and dynamics model (1979)[17]. The ocean and ice modules of the model both adopted the *C* grid, which is convenient for their coupling; the horizontal grid uses curvilinear orthogonal grid for higher model resolution and better handling of the oddity issue of the pole. In addition, the main part of the paper describes the grid generation techniques for the model and its major parameterization schemes.

On this basis, part of the simulation result—a climatology simulation and Arctic sea ice simulation for 2007—is presented in the paper. As comparison with observation data shown, the regional ice-ocean coupled model described in this paper can basically capture the basic characteristics of Arctic sea ice change and thus could be used in more advanced simulation and research on issues related to Arctic ice-ocean cou-

pling.

Acknowledgements This study was supported by the National Science and Technology Support Program of China (Grants No. 2006BAB18B03) and the Polar Science Strategic Research Foundation of China(Grants No. 20080223).

References

[1] Comiso J(2002): A rapidly declining perennial sea ice cover in the Arctic, Geophys. Res. Lett., 29, 1956, doi:10.1029/2002GL015650.
[2] Comiso J, Parkinson C, Gersten R, *et al*. (2008): Accelerated decline in the Arctic seaice cover, Geophys. Res. Lett., 35, L01703, doi:10.1029/2007GL031972.
[3] Nghiem S, Rigor I, Perovich D, Clemente-Colón P, Weatherly J and Neumann G (2007): Rapid reduction of Arctic perennial sea ice, Geophys. Res. Lett., 34, L19504, doi: 10.1029/2007GL031138.
[4] Steele M, Ermold W and Zhang J(2008): Arctic Ocean surface warming trends over the past 100 years, Geophys. Res. Lett., 35, L02614, doi:10.1029/2007GL031651.
[5] Richter-Menge J, Overland J, Proshutinsky A, *et al*. (2006): State of the Arctic report. NOAA OAR Special Report. Seattle: NOAA/OAR/PMEL.
[6] IPCC Forth Assessment Report. Climate Change(2007): The physical science basis. Solomon S., D. Qin, M. Manning, *et al*. Eds., Cambridge University Press, UK, 996.
[7] Meier W, Stroeve J, Fetterer F (2007): Whither Arctic sea ice? A clear signal of decline regionally, seasonally and extending beyond the satellite record, Ann. Glac., 46: 428-434.
[8] Chen LQ, Zhao JP, Bian LG, *et al*. (2003): Study on key processes affecting rapid changes in the Arctic. Chinese Jounal of Polar Science,15(4): 283-302 (In Chinese).
[9] Ebert EE and Curry JA (1993): An intermediate one-dimensional thermodynamic sea ice model for investigating ice-atmosphere interactions. J. Geophys. Res., 98: 10085-10109.
[10] Maslanik J, Fowler C, Stroeve J, *et al*. (2007): A younger, thinner Arctic ice cover: Increased potential for rapid, extensive sea-ice loss, Geophys. Res. Lett., 34, L24501, doi: 10.1029/2007GL032043.
[11] Perovich DK, Richter-Menge JA, Jones KF and Light B (2008): Sunlight, water, and ice: Extreme Arctic sea ice melt during the summer of 2007, Geophys. Res. Lett., 35, L11501, doi:10.1029/2008GL034007.
[12] Kauker F, Kaminski T, Karcher M, *et al*. (2009): Adjoint analysis of the 2007 all time Arctic sea-ice minimum, Geophys. Res. Lett., 36, L03707, doi:10.1029/2008GL036323.
[13] Zhang J, Rothrock DA and Steele M (2000): Recent changes in Arctic sea ice: The interplay between ice dynamics and thermodynamics. J. Climate, 13:3099-3114.
[14] Zhang J and Rothrock DA (2005): The effect of sea-ice rheology in numerical investigations of climate, J. Geophys. Res., 110, C08014, doi:10.1029/2004JC002599.
[15] Lindsay RW, Zhang J, Schweiger AJ, Steele MA and Stern H (2009): Arctic sea ice retreat in 2007 follows thinning trend. J. Clim., 22, 165-176, doi: 10.1175/2008JCLI2521.
[16] Menemenlis D, Campin JM, Heimbach P, Hill C, Lee T, Nguyen A, Schodlock M and Zhang H (2008): ECCO2: High resolution global ocean and sea ice data synthesis. Mercator Ocean Quarterly Newsletter, 31:13-21.
[17] Hibler III W D(1979): A dynamic thermodynamic sea ice model. J. Phys. Oceanogr. 9:815-846.
[18] Adcroft A, Campin JM, *et al*. MITgcm User Manual. MIT Department of EAPS. Cambridge, MA 02139-4307.
[19] Winton M(2000): A reformulated three-layer sea ice model. J. Atmos. Ocean. Technol., 17: 525-531.
[20] Parkinson CL and Washington WM (1979): A large-scale numerical model of sea ice. J. Geophys.

Res., 84:311-337.

[21] Zhang J, Hibler III WD, Steele M and Rothrock DA (1998): Arctic ice-ocean modeling with and without climate restoring. J. Phys. Oceanogr., 28:191-217.

[22] Adcroft A and Campin JM (2004): Re-scaled height coordinates for accurate representation of free-surface flows in ocean circulation models, Ocean Modelling, 7: 269-284.

[23] Campin JM and Adcroft A (2008): Sea ice-ocean coupling using a rescaled vertical coordinate $z*$. Ocean Modeling, 24:1-14.

[24] Proshutinsky A, Yang J, Krish_eld R, Gerdes R, *et al*. (2005): Arctic Ocean study: Synthesis of model results and observations. EOS, 86: 378-381.

[25] Nguyen AT, Menemenlis D and Kwok R (2009): Improved modeling of the Arctic halocline with a subgrid-scale brine rejection parameterization, J. Geophys. Res., 114, C11014, doi:10.1029/2008JC005121.

[26] Gent PR and McWilliams JC (1990): On parameterizing vertical mixing of momentum in non-eddy-resolving ocean models. J. Physics. Oceanogr., 20:1634-1637.

[27] Redi MH(1982): Oceanic isopycnal mixing by coordinate rotation. J. Physics. Oceanogr., 12: 1154-1158.

[28] Visbeck M, Marshall J, Haine T and Spall M (1997): Specification of eddy transfer coefficients in coarse-resolution ocean circulation models, J. Phys. Oceanogr., 27:381-402.

[29] Maslowski W, Kinney JC, Marble DC, *et al*. (2008): Towards eddy-resolving models of the Arctic Ocean. Geophysical Monograph Series, 177:241-264.

[30] Watanabe E and Hasumi H(2009): Pacific water transport in the western Arctic ocean simulated by an eddy-resolving coupled sea ice-ocean model. Journal of Physical Oceanography, DOI: 10.1175/2009JPO4010.1